Eur Radiol (2005) 15: 1361–1368
DOI 10.1007/s00330-005-2664-6

Eija Pääkkö
Heli Reinikainen
Eija-Leena Lindholm
Tarja Rissanen

Low-field versus high-field MRI in diagnosing breast disorders

Received: 5 August 2004
Revised: 17 December 2004
Accepted: 28 December 2004
Published online: 12 February 2005

E. Pääkkö (✉) · H. Reinikainen · E.-L. Lindholm · T. Rissanen
Department of Diagnostic Radiology,
University of Oulu,
Kajaanintie 50, PL 50,
90029 Oulu, Finland
e-mail: eija.paakko@oulu.fi
Tel.: +358-8-3152463
Fax: +358-8-3152112

Abstract We evaluated the performance of low-field MRI in breast disorders by comparing it with high-field MRI and biopsy results. Twenty-eight consecutive patients who were able to undergo two magnetic resonance examinations on following days were examined by high-field and low-field MRI. After T1-weighted sagittal images had been obtained a dynamic 3D axial study was performed followed by the acquisition of contrast-enhanced T1-weighted sagittal images. The images were analyzed separately by two radiologists paying attention to lesion morphology and enhancement kinetics. Six patients had problems in both breasts (34 breasts studied). The results were compared with biopsy results of 27 breasts. There were 16 malignant lesions, two fibroadenomas and nine other benign lesions. The inter-magnetic-resonance-scanner κ value was 0.77 (substantial agreement), while the interobserver κ value was 0.86 and 0.81 at low and high field, respectively (excellent agreement). The sensitivity was 100 and 100%, the specificity was 82 and 73% and the accuracy was 93 and 89% at low and high field, respectively. The mean lesion size was 2 cm and the smallest malignant lesion was 8 mm in diameter. Low-field MRI is a promising tool for breast imaging. Larger materials and smaller lesions are needed to evaluate its true sensitivity and specificity.

Keywords Breast · Magnetic resonance imaging · Low field

Introduction

Since its introduction at the end of the 1980s contrast-enhanced MRI of the breast has gained an increasing role in diagnosing breast tumors [1, 2]. The sensitivity of high-field MRI has approached 100%, while the specificity has been more variable in different studies [3–8]. It has been used as a problem-solving tool when mammography and ultrasonography have been inconclusive or when more precise preoperative diagnosis of multicentricity or multifocality has been considered important [9–12]. It has also been used in postoperative surveillance after conservative surgery and in searching for primary cancer in patients with axillary node metastases [13–15]. MRI has also been used in image-guided procedures, such as biopsies and wire localization, in cases where the suspected lesion is visible only by MRI [16–18].

Low-field MRI is an appealing concept in breast imaging owing to lower equipment costs and patient-friendly, open design. The open configuration is also of benefit when considering image-guided procedures [19]. However, the lower signal-to-noise ratio, longer imaging times and the unavailability of fat suppression based on chemical shift may have decreased the interest in low-field MRI of the breast. There is a preliminary report comparing high-field (1.0 T) with low-field (0.2 T) MRI in the detection of breast lesions in 11 patients [20]. All lesions that were considered suspect at high field were also identified at low field. Our purpose was to explore the feasibility of a modern low-field magnetic resonance scanner in diagnosing breast disorders by comparing its performance with that of a high-field unit

and with biopsy results. Without previous experience in low-field breast imaging our goal was, in particular, to find out whether the findings observed at high field in an unselected patient material could be repeated at low field. We were especially interested in the reproducibility of the findings to justify image-guided procedures at low field.

Patients and methods

Twenty-eight consecutive patients who were able to undergo two breast magnetic resonance examinations on following days were collected over 2 years. First the patients were examined by high-field MRI (1.5 T, Signa Echo-Speed, General Electric Medical Systems) and the following day by low-field MRI (0.23 T Panorama Power, Philips Medical Systems). The mean age of the patients was 52 years (range 30–74 years). Six patients had problems in both breasts and accordingly 34 breasts were studied. The reason for the examination was a palpable lump in 12 breasts, an inconclusive mammography in 14 breasts, suspicious calcifications detected by mammography in seven breasts and an axillary node metastasis with a normal mammography in one patient (counted as one breast). One of the patients had undergone conservative surgery and radiotherapy owing to lobular carcinoma 5 years earlier.

The patients were imaged in the prone position with a double breast coil. After T1-weighted sagittal images had been obtained a dynamic 3D axial study was performed. One axial series was obtained before contrast injection. At high field the dynamic series was repeated eight times and at low field six times after contrast injection [power injector at high field 3 ml/s, manual injection (approximately in 10 s) at low field]. The dose of intravenous contrast agent (Magnevist, Schering) was 0.2 mmol/kg at high field, with a maximum of 30 ml. Accordingly the injected dose was 20–30 ml, with a mean of 26 ml. At low field a dose of 30 ml was used for patients who weighted over 50 kg and 25 ml for those who weighted 50 kg or less (one patient). The contrast injection was followed by a saline flush (10 ml at high field, 20 ml at low field). The imaging time for one dynamic axial series was 43 s at high field and 60 s at low field. After the dynamic series contrast-enhanced T1-weighted sagittal images were obtained again. The specifications for the examinations are presented in Table 1.

At high field, chemical-shift fat saturation was used to facilitate lesion detection. The images were further analyzed using a workstation (Advantage Windows, GE Medical Systems) with a computer-assisted program (Functool) to get the maps of the maximum slope of increase for each slice of the dynamic series. This program allowed color-coded images in which pathological enhancement was easy to detect. At low field, VIA 2.0 software (Philips Medical Systems) was used for postprocessing. Image subtraction was performed for lesion detection in the dynamic series. In the postcontrast sagittal T1-weighted 3D field echo series postprocessing fat saturation was performed based on the phase-difference water–fat imaging method [21].

The images were analyzed separately by two radiologists (E.P. and H.R.) 3–25 months after the studies had been performed. Both radiologists analyzed the studies performed at high field first and approximately 3 months later the studies performed at low field. The radiologists were unaware of the biopsy results. The images were analyzed by paying attention to masses and abnormal enhancement. Lesion morphology and enhancement kinetics were analyzed in all lesions that were suspicious from MRI. Time–signal intensity curves were obtained from enhancing lesions by placing multiple regions of interest (ROIs) at the sites with maximum enhancement, after which the most suspicious curve was selected. The size of the ROI varied according to the size of the lesion and the area of maximum enhancement. In small lesions the ROI included the whole lesion, while in larger lesions the area showing the greatest enhancement was included. Lesions with a washout time–signal intensity curve or/and spiculated margins or rim enhancement were considered malignant (Fig. 1). Lesions with ill-defined margins and a plateau curve were also considered malignant, while ill-defined lesions with a sustained type of curve were characterized as indeterminate. Well-defined lesions with a plateau curve were also considered indeterminate. Lesions with well-defined margins and a sustained-type time–signal intensity curve were classified as benign (Fig. 2).

Table 1 Breast MRI protocols used at 0.23 and 1.5 T

	TR (ms)	TE (ms)	TI (ms)	FA (°)	Thk (mm)	Gap (mm)	NSA	FOV (cm)	Matrix	TA (min)
0.23 T										
FE 3D T1 sagittal	25	8	–	30	3.0–3.5	–	1	25	256×256	5:48
FE 3D T1 transverse	13	5.2	–	20	3.0–4.0	–	1	35–38	192×192	1:00
1.5 T										
SE T1 sagittal fs	600	9	–	90	3.0–5.0	0.5	2	16–22	256×224	4:32
efgre 3D transverse fs*	6.1	1.3	32	30	2.6–4.0	–	1	28–40	256×128	0:43

TR repetition time, *TE* echo time, *TI* inversion time, *FA* flip angle, *Thk* section thickness, *Gap* intersection gap, *NSA* number of signals averaged, *FOV* field of view, *TA* acquisition time, *FE* field echo, *SE* spin echo, *fs* fat-suppressed, *efgre* enhanced fast gradient echo, *fs** fat saturation with spectral inversion at lipids (*SPECIAL*)

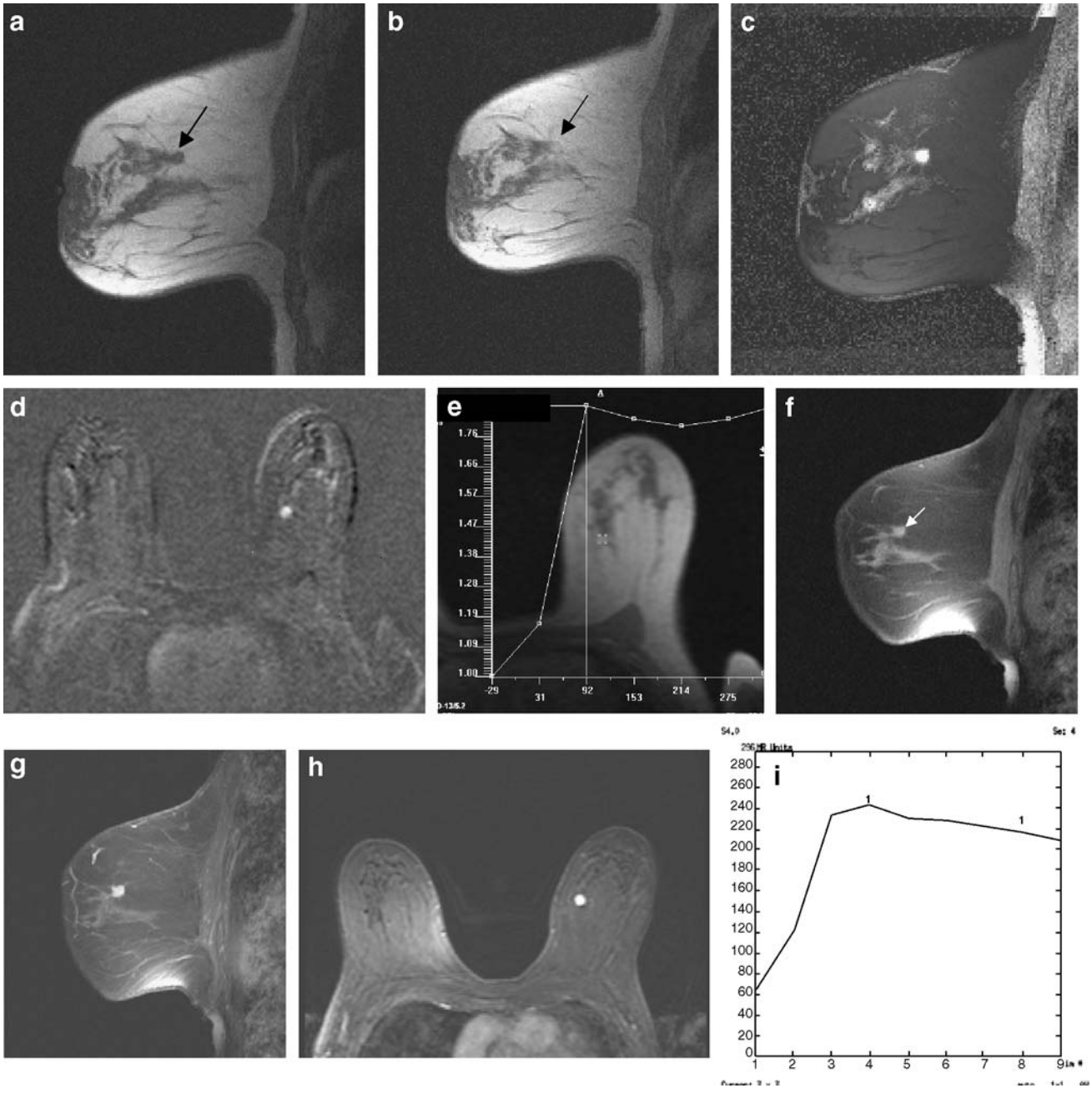

Fig. 1 Images obtained with low-field and high-field MRI of a 72-year-old woman with a suspicious lesion from mammography. A small, spiculated lesion is observed on sagittal T1-weighted images before contrast injection (**a** low field, **f** high field). At low field, enhancement of the lesion is largely obscured by surrounding fat (**b**), but is clearly visible after fat suppression (**c**) and is comparable to the contrast-enhanced fat-suppressed image obtained at high field (**g**). The lesion is also well seen on a subtracted image from the dynamic contrast-enhanced series at low field (**d**) and the fat-suppressed dynamic image at high field (**h**). At low field the dynamic time–signal intensity curve shows washout with a slight later increase in signal intensity (**e**), while at high field a more typical washout curve is observed (**i**). The MRI findings are compatible with a malignant lesion which was confirmed by biopsy showing invasive lobular cancer. There is also some enhancement in the normal breast parenchyma, especially in **c**; however, no evidence of multifocal disease was observed.

κ statistics were used to compare the performance between the magnetic resonance scanners and readers [22]. In cases of discrepancy between the readers a consensus reading was performed after all high-field and low-field studies had been analyzed.

Lesion conspicuity in the various sequences was analyzed and rated from 0 to 4: 0 for not seen, 1 for poor, 2 for

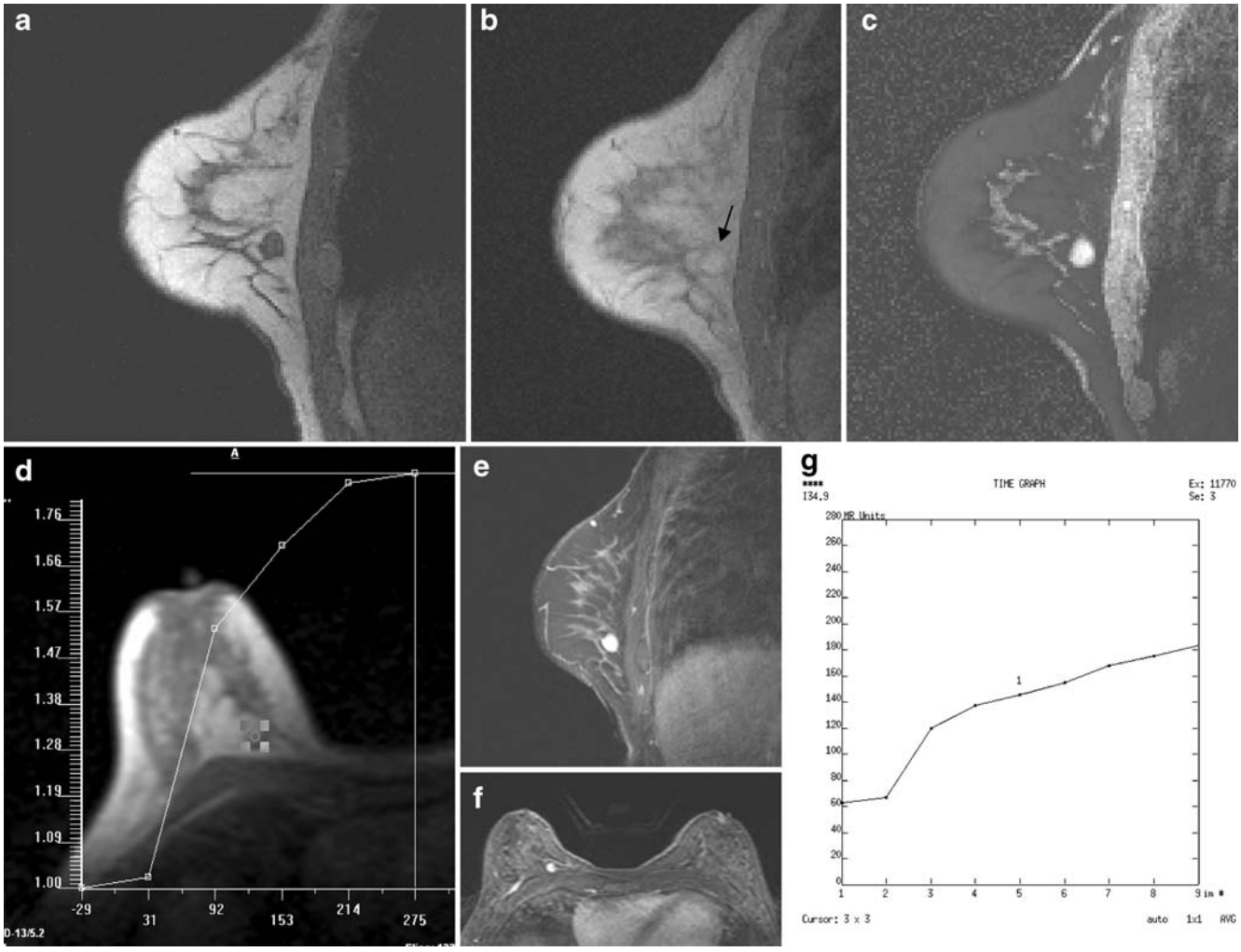

Fig. 2 A 45-year-old patient had subjective symptoms in the right breast and mammography showed a new well-defined lesion that was not visible from the previous mammography. At low-field MRI a well-defined lesion was observed on precontrast images (**a**). After contrast injection the lesion enhanced and is barely visible on a 3D sagittal slice (**b**) but is obvious on a fat-suppressed image (**c**). The dynamic time–signal intensity curve shows a constant increase in signal intensity during the 7-min acquisition (**d**). The lesion also shows the same features at high field (**e** fat-suppressed postcontrast T1-weighted image, **f** fat-suppressed dynamic image, **g** dynamic time–signal intensity curve). The lesion was classified as benign by MRI and biopsy showed a fibroadenoma. Besides the round enhancing tumor there is an elongated enhancing structure in **f** which represents a vein.

moderate, 3 for good, 4 for excellent. At high field the three imaging sequences were analyzed, while at low field lesion conspicuity was also assessed from the subtracted and post-processed fat-suppressed images. At high field the contribution of the computer-assisted program (maximum slope of increase) to lesion detection was also analyzed and was rated from 0 to 3: 0 for not seen, 1 for seen as well as on the dynamic series, 2 for helped in lesion detection, 3 for crucial in lesion detection. The overall image quality, including motion artifacts, was analyzed and classified as insufficient, poor, fair or good. The uniformity of fat suppression was also rated as poor, fair or good.

The relative enhancement of the lesions was calculated, although it was not used in lesion characterization, by using the formula relative SI $(\%) = \left(\mathrm{SI}_{\mathrm{post}} - \mathrm{SI}_{\mathrm{pre}} / \mathrm{SI}_{\mathrm{pre}}\right) \times 100$, where $\mathrm{SI}_{\mathrm{pre}}$ is the precontrast signal intensity and $\mathrm{SI}_{\mathrm{post}}$ the maximal signal intensity within 2 min from the beginning of the dynamic series. Confidence intervals (CI) of 95% were calculated for the enhancement ratios.

Informed consent was obtained from the patients. The study was approved by the ethical committee of the university hospital.

Results

Histological confirmation was available in 25 breasts including 20 operative specimens and five core biopsies,

Table 2 The performance of low-field versus high-field MRI in analyzing breast lesions in 34 breasts based on consensus reading of the two observers

Low field	High field				Total
	Normal	Benign	Indeterminate	Malignant	
Normal	5	1			6
Benign		7	1	2	10
Indeterminate		1	1		2
Malignant				16	16
Total	5	9	2	18	34

while in two cases a fine needle biopsy was obtained. The findings included two fibroadenomas, nine other benign lesions (six fibrocystic mastopathy, three fibrosis, including one postoperative scar) and 16 malignant lesions (three ductal carcinoma in situ, eight invasive ductal carcinoma, four invasive lobular carcinoma and one invasive mucinous carcinoma). Three biopsies were performed using MRI guidance.

The size of the lesions varied from 6 to 70 mm, with a mean of 20 mm. Seven lesions were 10 mm or smaller. The smallest malignant lesion detected was an 8-mm invasive lobular carcinoma (Fig. 1).

Comparison between the performance of the magnetic resonance scanners is shown in Table 2. The interscanner κ value was 0.77 (substantial agreement). The differences between the evaluations of the two readers is shown in Tables 3 and 4. The interobserver κ value was 0.86 at low field and 0.81 at high field (excellent agreement).

The MRI results at low and high field compared with biopsy results are shown in Table 5. The sensitivity, specificity and accuracy were 100, 82 and 93% at low field compared with 100, 73 and 89% at high field. There were two false-positives at low field and three at high field when the indeterminate cases were included. At low field one false-positive case had a 3-cm indistinct area of enhancement with a sustained curve which was considered indeterminate. Biopsy showed fibrocystic mastopathy. The other false-positive at low field was a fibroadenoma (12 mm) with indistinct margins and a plateau curve. This same fibroadenoma was considered indeterminate also at high field and hence was classified as false-positive. At high field the two other false-positives represented fibrocystic

Table 3 Comparison of the evaluation of the two observers in diagnosing breast disorders in 34 breasts from low-field MRI

Observer 2	Observer 1				Total
	Normal	Benign	Indeterminate	Malignant	
Normal	5				5
Benign	1	10	1		12
Malignant			1	16	17
Total	6	10	2	16	34

Table 4 Comparison of the evaluation of the two observers in diagnosing breast disorders in 34 breasts from high-field MRI

Observer 2	Observer 1				Total
	Normal	Benign	Indeterminate	Malignant	
Normal	5				5
Benign		8	1		9
Indeterminate				2	2
Malignant			1	17	18
Total	5	8	2	19	34

mastopathy which were small lesions (7 and 12 mm) with a washout curve and were considered malignant. There were no false-negative cases. No multifocal cancers were detected.

In the three cases with biopsy-confirmed fibrosis no pathological enhancement was observed from MRI. Mammography showed that one of these patients had microcalcifications and a core biopsy was performed. Mammography showed that another had a dense breast and ultrasonography indicated architectural distortion, which was evaluated by core biopsy. The third patient had a postoperative scar, which was also visible by MRI as a stellate lesion with minor enhancement and a sustained type of time–signal intensity curve. It was correctly classified as a benign finding.

In the seven cases where biopsy confirmation was not obtained, MRI did not reveal any abnormality and further examinations were considered unnecessary. The patients were referred back to normal observation for their age. The reason for MRI in all these cases was an inconclusive mammography.

When analyzing the conspicuity of the lesions a dynamic fat-saturated transverse series at high field was considered the best, reaching a mean value of 3.2 (Table 6). At low field, lesions were best seen in the subtracted images, where the mean value was 2.4. On sagittal contrast-enhanced post-processed fat-saturated images at low field, lesion conspicuity was equal to that in fat-saturated sagittal postcontrast images at high field and reached a mean value of 2.2. At

Table 5 Findings from low-field and high-field MRI of breast lesions compared with biopsy results in 27 breasts

	Biopsy result	
	Benign (n=11)	Malignant (n=16)
Low-field MRI		
Benign	9	
Indeterminate	2	
Malignant		16
High-field MRI		
Benign	8	
Indeterminate	1	
Malignant	2	16

Table 6 Lesion conspicuity in different sequences and postprocessed images from low-field and high-field MRI on a scale 0–4, where 0 is not seen, 1 is poor, 2 is moderate, 3 is good and 4 is excellent. The values are means.

	Low field	High field
T1 sagittal[a]	1.0	1.2
T1 sagittal[a]+C	1.3	2.2
3D dynamic transverse[b]+C	1.8	3.2
T1 sagittal plus postprocessing fat saturation	2.2	–
Subtracted images	2.4	–

C intravenous contrast agent
[a]3D FE series at low field, 2D SE series with fat saturation at high field
[b]SPECIAL fat saturation at high field

high field the computer-assisted program allowing color-coded images of the maximum slope of increase was considered to be helpful in lesion detection in nine observations and to be crucial in lesion detection in another nine of 68 observations from 34 breasts (13%) (including the observations of both radiologists). These included especially cases where fat saturation on the dynamic contrast-enhanced 3D enhanced fast gradient echo (efgre) series was suboptimal making lesion detection difficult. In the rest of the cases lesions were seen as well on the fat-saturated postcontrast 3D efgre images.

Overall image quality was equal in the sagittal images at low field compared with those at high field and no imaging series were considered to be insufficient for diagnostics (Table 7). When considering the most important series in lesion detection, i.e., subtracted images at low field and fat-saturated 3D efgre images at high field, image quality was better at high field, where good image quality was observed in 69% of cases compared with 35% of cases at low field. The uniformity of fat suppression was better in

Table 7 Overall image quality and the uniformity of fat suppression in various sequences for low-field and high-field MRI of breast lesions

	Image quality			Fat suppression		
	Poor	Fair	Good	Poor	Fair	Good
Low field						
FE 3D T1 sagittal	–	6	94	na	na	na
FE 3D T1 sagittal+C	–	10	90	1*	91*	8*
FE 3D T1 transverse	–	4	96	na	na	na
Subtracted images	2	63	35	na	na	na
High field						
SE T1 sagittal fs	–	7	93	6	43	51
SE T1 sagittal fs+C	–	7	93	1	24	75
Efgre 3D transverse fs	2	29	69	13	40	47

The numbers are percentages.
na not applicable
*Fat suppression performed by postprocessing

postcontrast sagittal series at high field compared with postprocessed fat-saturated sagittal images at low field, with good fat suppression in 75 and 8%, respectively.

At low field the mean relative enhancement of benign lesions was 66% (range 18–134%), 95% CI 14–118% and of malignant lesions it was 124% (range 102–147%), 95% CI 70–147%. At high field the figures were 148% (range 32–376%), 95% CI-22–318% and 369% (range 116–573%), 95% CI 295–444%, respectively.

Discussion

Breast MRI has been shown to be a valuable and sensitive tool in diagnosing breast diseases [6, 7, 23, 24]. There are a number of factors limiting its use as an adjunct to conventional methods such as mammography and ultrasonography. One of the limiting factors is the high cost of high-field MRI. Another factor is the lack of appropriate MRI biopsy guiding methods which are needed when evaluating lesions observed only by MRI. A low-field open MRI unit could be a solution to these problems: lower equipment costs lead to lower prices and the open configuration allows easy access in breast biopsies. High-quality diagnostic imaging with a sensitivity and specificity comparable to high-field MRI, however, is the prerequisite if low-field MRI is to play a role in diagnosing breast diseases. In a preliminary study low-field MRI showed all suspect breast lesions visualized by high-field MRI in 11 patients [20].

We wanted to evaluate whether the results obtained with high-field breast imaging could be repeated with low-field MRI in an unselected patient population referred for breast MRI. In this study of 28 patients with 34 breasts examined we found similar performance of low-field and high-field MRI (Table 2), and the sensitivity and specificity were also comparable in the 27 breast lesions with biopsy confirmation (Table 5). Because of the small amount of material, sensitivity and specificity may not be reliable estimates of the performance of the scanners. However, we wanted to use these estimates to help make a comparison between the scanners and the sensitivity and specificity values seemed to parallel previous experience with high-field units [4–6, 12]. We want to emphasize that our results do not represent the true sensitivity and specificity of low-field MRI.

Differential diagnosis of MRI-visible breast lesions includes analysis of lesion morphology and the dynamics of contrast enhancement [5, 7]. However, with current technology it is difficult to perform a study with good temporal and spatial resolution. The former means fast scanning after contrast agent injection and is a prerequisite for detailed time–signal intensity curves. Good spatial resolution, on the other hand, means longer imaging times, making detailed architectural analysis of lesion borders possible. In our study we emphasized good temporal resolution at the cost of spatial resolution in the dynamic series. T1-weighted sagittal images with better spatial resolution were obtained

several minutes after contrast injection. During this time the contrast agent will have entered the glandular tissue around the enhancing lesion obscuring lesion margins and together with the washout phenomena making detailed morphological analysis difficult [25]. A solution to this controversy between temporal and spatial resolution has been suggested by combining T1-weighted 3D gradient echo imaging at low and high resolution. Low-resolution faster scanning is performed for a limited time (e.g., 3 min) after contrast injection, followed immediately by high-resolution imaging giving the required spatial resolution [25].

Good spatial resolution is also a prerequisite in MRI to find small enhancing lesions. The smallest lesions observed in this study with low-field and high-field MRI were 6 mm in diameter and the smallest malignant lesion found was 8 mm. Although we did not use the same resolution in the same lesions between low-field and high-field imaging, it seems that the spatial resolution used here (pixel size 1.8×1.8–2.0×2.0 mm for low field and 1.1×2.2–1.6×3.1 mm for high field, with 2.6–4-mm slice thickness in the dynamic series) was good enough to detect lesions that are of relevant size to consider biopsy using magnetic resonance guidance [18]. However, the number of patients with small lesions was small in our sample. A larger number of patients and more small lesions, which are the target of breast MRI, are needed to evaluate the true performance of low-field MRI in breast imaging.

When considering the imaging protocols between low and high field there were no major differences in imaging times between the scanners, although obtaining T1-weighted sagittal images at low field took more than 1 min longer (Table 1). At low field, 3D field echo imaging was used in the sagittal series, while 2D spin echo was used at high field. 3D imaging was chosen at low field to compensate for the lower signal-to-noise ratio and to give better spatial coverage of the whole breast. 3D sequences also offer better T1 contrast and are more sensitive to the T1-shortening effects of gadolinium, which are lower at low field. 3D imaging was used in both scanners during the dynamic series, where imaging speed is also crucial.

Lesion conspicuity at high field was in general better than at low field (Table 6), except in fat-suppressed contrast-enhanced T1-weighted sagittal images (postprocessed at low field) which reached the same conspicuity value. General image quality was also poorer in subtracted dynamic images at low field compared with the quality of the dynamic fat-suppressed images at high field. Image subtraction is very prone to patient movement and even slight movement during the comparatively long dynamic series (7×1 min) may cause significant artifacts and make the detection of small lesions difficult. Uniformity of fat suppression was also inferior in postprocessed images at low field compared with that at high field (Table 7). Breast diagnostics from MRI is based on a combination of imaging sequences and relevant results were obtained in spite of lower image quality at low field as seen in the comparable performance of the scanners (Tables 2, 5).

Although the computer-assisted program at high field allowing color-coded maps of the maximum slope of increase did not play a major role in lesion detection when compared with the dynamic fat-suppressed 3D efgre series, it was considered to be very helpful in lesion analysis. It was felt that detecting enhancing lesions was very fast on the maps. It was also fast to screen the time–signal intensity curves in the lesions because placing the cursor in different areas of the enhancing lesion allowed a quick survey of the time–signal intensity curves of the pixels. After that ROIs of different size were placed over the lesion in the most suspicious areas to get more representative curves for the final analysis.

The lesion enhancement ratio is one aspect frequently used in lesion characterization [6, 7]. It has been observed, however, that there may be considerable overlapping between the enhancement ratios of benign and malignant lesions and no uniform criteria can be achieved because of different types of scanners, imaging protocols and doses of the contrast agent [6, 23]. We calculated the enhancement ratios, although we did not use them in differential diagnosis, on the basis of previous experience [26]. As expected, the lesions enhanced to a higher degree at high field compared with low field: there was approximately a twofold difference in benign lesions (mean relative enhancement of 148% at high field and 66% at low field) and a threefold difference in malignant lesions (mean relative enhancement of 369% at high field and 124% at low field). Our results are in accordance with phantom measurements considering field strength dependence of MRI contrast enhancement [27]. It was shown that the relative enhancement has a strong dependence on the magnetic field strength and was greater at high field strengths. It was estimated that malignant breast tumors show an almost 2 times lower enhancement ratio at low field (0.2 T) than at high field (1.5 T). It was concluded that this might lead to misclassification if criteria established at high field are used to classify lesions detected at low field.

There are several limitations in our study in addition to the small patient material. First, the comparability of data at high and low field may be influenced by the different doses of the contrast medium (0.2 mmol/kg with a maximum of 30 ml and a mean of 26 ml at high field compared with 30 ml, except for 25 ml in one patient, at low field). We used the higher dose at low field to compensate for the decreased sensitivity to enhancement. This may not have had a major impact, however, as the expected differences in the enhancement ratios between low and high field were preserved [27] and the performances of the scanners were comparable in detecting and characterizing lesions (Tables 2, 5). Second, we counted the breasts rather than the lesions, which would have helped in more precise correlation of the findings. Counting lesions was not practical, however, because many patients were referred to MRI

owing to inconclusive mammography combined with subjective symptoms and unclear palpation findings without a definitive lesion that should have been evaluated by MRI. Third, the examinations at high field were evaluated first and approximately 3 months later at low field, which may have had some favorable impact on low-field analyses. There was a practical reason because the workstation at high field was available more often than the working console at low field.

In conclusion, on the basis of our experience with a relatively small number of patients an 0.23-T open magnetic resonance system was feasible and showed comparable performance with a high-field unit for various breast lesions. These results do not, however, represent the true sensitivity and specificity of low-field MRI and larger patient materials with smaller lesions are needed. In reproducing the findings obtained at high-field, low-field open MRI has potential in image-guided breast procedures [19, 20].

References

1. Heywang SH, Wolf A, Pruss E, Hilbertz T, Eiermann W, Permanetter W (1989) MR imaging of the breast with Gd-DTPA: use and limitations. Radiology 171:95–103
2. Kaiser WA, Zeitler E (1989) MR imaging of the breast: fast imaging sequences with and without Gd-DTPA. Preliminary observations. Radiology 170:681–686
3. Stomper PC, Herman S, Klippenstein DL et al (1995) Suspect breast lesions: findings at dynamic gadolinium-enhanced MR imaging correlated with mammographic and pathologic features. Radiology 197:387–395
4. Nunes LW, Schnall MD, Orel SG et al (1997) Breast MR imaging: interpretation model. Radiology 202:833–841
5. Liu PF, Debatin JF, Caduff RF, Kacl G, Garzoli E, Krestin GP (1998) Improved diagnostic accuracy in dynamic contrast enhanced MRI of the breast by combined quantitative and qualitative analysis. Br J Radiol 71:501–509
6. Kuhl CK, Mielcareck P, Klaschik S et al (1999) Dynamic breast MR imaging: are signal intensity time course data useful for differential diagnosis of enhancing lesions? Radiology 211:101–110
7. Baum F, Fischer U, Vosshenrich R, Grabbe E (2002) Classification of hypervascularized lesions in CE MR imaging of the breast. Eur Radiol 12:1087–1092
8. Obdeijn IM, Kuijpers TJ, van Dijk P, Wiggers T, Oudkerk M (1996) MR lesion detection in a breast cancer population. J Magn Reson Imaging 6:849–854
9. Lee CH, Smith RC, Levine JA, Troiano RN, Tocino I (1999) Clinical usefulness of MR imaging of the breast in the evaluation of the problematic mammogram. Am J Roentgenol 173:1323–1329
10. Weinstein SP, Orel SG, Heller R et al (2001) MR imaging of the breast in patients with invasive lobular carcinoma. Am J Roentgenol 176:399–406
11. Orel SG, Schnall MD, Powell CM et al (1995) Staging of suspected breast cancer: effect of MR imaging and MR-guided biopsy. Radiology 196:115–122
12. Fischer U, Kopka L, Grabbe E (1999) Breast carcinoma: effect of preoperative contrast-enhanced MR imaging on the therapeutic approach. Radiology 213:881–888
13. Muuller RD, Barkhausen J, Sauerwein W, Langer R (1998) Assessment of local recurrence after breast-conserving therapy with MRI. J Comput Assist Tomogr 22:408–412
14. Viehweg P, Heinig A, Lampe D, Buchmann J, Heywang-Kobrunner SH (1998) Retrospective analysis for evaluation of the value of contrast-enhanced MRI in patients treated with breast conservative therapy. Magma 7:141–152
15. Morris EA, Schwartz LH, Dershaw DD, van Zee KJ, Abramson AF, Liberman L (1997) MR imaging of the breast in patients with occult primary breast carcinoma. Radiology 205:437–440
16. Heywang-Kobrunner SH, Huynh AT, Viehweg P, Hanke W, Requardt H, Paprosch I (1994) Prototype breast coil for MR-guided needle localization. J Comput Assist Tomogr 18:876–881
17. Orel SG, Schnall MD, Newman RW, Powell CM, Torosian MH, Rosato EF (1994) MR imaging-guided localization and biopsy of breast lesions: initial experience. Radiology 193:97–102
18. Kuhl CK, Morakkabati N, Leutner CC, Schmiedel A, Wardelmann E, Schild HH (2001) MR imaging-guided large-core (14-gauge) needle biopsy of small lesions visible at breast MR imaging alone. Radiology 220:31–39
19. Ojala R, Sequeiros RB, Klemola R, Vanhala E, Jyrkinen L, Tervonen O (2002) MR-guided bone biopsy—preliminary report of a new guiding method. J Magn Reson Imaging 15:82–86
20. Sittek H, Perlet C, Herrman K, Linsmeier E, Kolem H, Untch M, Kessler M, Reiser M (1997) MR mammography. Preoperative marking of non-palpable breast lesions with the magnetom open at 0.2 T. Radiologe 37:685–691
21. Palosaari K, Tervonen O (2002) Post-processing water-fat imaging technique for fat suppression in a low-field MR imaging system, evaluation in patients with rheumatoid arthritis. Magma 15:1–9
22. Landis JR, Koch GG (1977) The measurement of observer agreement for categorical data. Biometrics 33:159–174
23. Orel SG, Schnall MD (2001) MR imaging of the breast for the detection, diagnosis and staging of breast cancer. Radiology 220:13–30
24. Sardanelli F, Iozelli A, Fausto A (2003) MR imaging of the breast: indications, established technique and new directions. Eur Radiol 13(Suppl 3):N28–N36
25. Vomweg TW, Teifke A, Kunz RP, Hintze C, Hlawatsch A, Kern A, Kreitner KF, Thelen M (2004) Combination of low and high resolution sequences in two orientations for dynamic contrast-enhanced MRI of the breast: more than a compromise. Eur Radiol 14:1732–1742
26. Reinikainen H, Paakko E, Suramo I, Paivansalo M, Jauhiainen J, Rissanen T (2002) Dynamics of contrast enhancement in MR imaging and power Doppler ultrasonography of solid breast lesions. Acta Radiol 43:492–500
27. Hittmair K, Turetschek K, Gomiscek G, Stiglblauer R, Schurawitzki H (1996) Field strength dependence of MRI contrast enhancement: phantom measurements and application to dynamic breast imaging. Br J Radiol 69:215–220